Oncogenic Ras Diverts a Host TNF Tumor Suppressor Activity into Tumor Promoter

Julia B. Cordero[1], **Juan P. Macagno**[1], **Rhoda K. Stefanatos**[1], **Karen E. Strathdee**[1], **Ross L. Cagan**[2], and **Marcos Vidal**[1,*]

[1]Beatson Institute for Cancer Research, Cancer Research UK. Garscube Estate, Switchback Road, Bearsden, Glasgow G61 1BD, UK

[2]Department of Developmental and Regenerative Biology, Annenberg 25-40, Mount Sinai Medical School, One Gustave L. Levy Place, Box 1020, NY 10029, USA

SUMMARY

The roles of inflammatory cytokines and the immune response in cancer remain paradoxical. In the case of tumor necrosis factor (TNF), there is undisputed evidence indicating both protumor and antitumor activities. Recent work in *Drosophila* indicated that a TNF-dependent mechanism eliminates cells deficient for the polarity tumor suppressors *dlg* or *scrib*. In this study, however, we show that in tumors deficient for *scrib* that also expressed the Ras oncoprotein, the TNF signal was diverted into a protumor signal that enhanced tumor growth through larval arrest and stimulated invasive migration. In this case, TNF promoted malignancy and was detrimental to host survival. TNF was expressed at high levels by tumor-associated hemocytes recruited from the circulation. The expression of TNF by hemocytes was both necessary and sufficient to trigger TNF signaling in tumor cells. Our evidence suggests that tumors can evolve into malignancy through oncogenic Ras activation and the hijacking of TNF signaling.

INTRODUCTION

The roles of mammalian tumor necrosis factor (TNF) as both protumor and antitumor are well documented. Initially, treatment with TNF induced necrotic death of subcutaneous murine tumors (Balkwill et al., 1986). On the contrary, later findings showed that TNF deficient mice are more resistant than wild-type to developing tumors (Moore et al., 1999). The molecular mechanisms determining such opposing roles of TNF remain largely unclear. One source of uncertainty is the undefined genetic composition and developmental history of the tumor models used.

The fruit fly *Drosophila melanogaster* is an excellent genetically tractable model system to address the complex cell interactions and genetic cooperation that lead to tumor formation and progression (Vidal and Cagan, 2006). Indeed, the discovery of *lethal giant larvae* (*lgl*) in *Drosophila* (Bridges and Brehme, 1944) provided founding evidence for the existence of tumor suppressor genes.

A significant body of work in *Drosophila* has uncovered the complex mechanisms underlying the role of tumor suppressors and oncogenes in tumorigenesis. Animals fully mutant for *lgl* and other polarity tumor suppressor genes from the "*scribble* group" such as *scribble* (*scrib*) and *disc large* (*dlg*) develop tumors within islands of polarized epithelia known as imaginal discs (Bilder and Perrimon, 2000; Humbert et al., 2008; Perrimon, 1988). On the contrary, discrete clonal patches of genotypically *scrib*$^{-/-}$ cells are eliminated by Jun N-terminal kinase (JNK)-dependent cell death (Brumby and Richardson, 2003). Nevertheless, overexpression of oncogenic Ras (*Ras^{V12}*) in discrete *scrib*$^{-/-}$ clones (*Ras^{V12}*; *scrib*$^{-/-}$) leads to invasive tumors (Pagliarini and Xu, 2003) in part due to a blockade of JNK-dependent death (Brumby and Richardson, 2005).

Although the JNK-dependent death of *dlg*- or *scrib*-deficient cells provides a mechanism to eliminate tumors, JNK also constitutes a pleiotropic signaling node with multiple roles in development, homeostasis, and the stress response. In the context of *Ras^{V12}*; *scrib*$^{-/-}$ tumors *Drosophila* JNK activation results in invasive cell migration (Igaki et al., 2006; Uhlirova and Bohmann, 2006) through the production of the matrix metallo-protease dMMP1 (Page-McCaw et al., 2003; Uhlirova and Bohmann, 2006).

Among the wide palette of cellular events leading to JNK activation is *dTNF/eiger* (*egr*). Egr is the sole *Drosophila* member of the TNF superfamily and its misexpression in imaginal disc cells results in JNK-dependent apoptosis (Igaki et al., 2002; Moreno et al., 2002). Recent work suggests that the immune system also plays a critical role in *Drosophila* tumor models: (1) hemocytes have been shown to associate to *Ras^{V12}*; *scrib*$^{-/-}$ tumors and negatively impact tumor growth in *scrib*$^{-/-}$ animals (Pastor-Pareja et al., 2008); and (2) JNK-dependent cell death in *scrib* or *dlg* clonal patches of cells requires *egr* (Igaki et al., 2009). The later suggests that the role of TNF as a "tumor death factor" is ancient and conserved from *Drosophila* to mammals.

Using a genetically defined tumor model we show that the "tumor promoting" role of mammalian TNF (Moore et al., 1999) is also conserved in *Drosophila*. We found that TNF acts as a tumor promoter in the context of *Ras^{V12}*; *scrib*$^{-/-}$ tumors. Furthermore, TNF was expressed by tumor-associated hemocytes and such expression was both necessary and sufficient for pathway activation in tumor cells. Our results provide what we believe to be novel mechanistic insights explaining the contrasting roles of the immune system in tumorigenesis and suggest a strong dependency on the genetic composition of the tumor.

RESULTS

TNF Is Required for dlg Cell Death and Epithelial Delamination

To further analyze the role of *egr* in cells deficient for tumor suppressors of the *scribble* group, we initially combined an *egr* loss of function mutant with an RNA-interference transgene targeting *dlg* (*dlg-IR*). This allowed control of gene expression by using the *gal4/UAS* system (Brand and Perrimon, 1993). *dlg-IR* resulted in decreased levels of the Dlg protein (see Figures S1 and S2 available online), phenocopied *dlg* mutants when ubiquitously expressed (Figure S4), and was rescued by coexpression of Dlg (Figure S2C). Expression of *dlg-IR* under the *decapentaplegic* (*dpp*) or *scalloped* (*sd*) promoters (*dpp > dlg-IR* or *sd > dlg-IR*) resulted in apoptosis (as assessed by caspase cleavage) (Figures 1A and S2B) and in an invasion-like phenotype in which cells delaminated and migrated away from the site of origin within the wing disc epithelium (Figures 1A and S1A). Despite these phenotypes most *dpp > dlg-IR* animals (91%, n = 81) (Figure S1G) survived to adulthood, displaying scars along the anterior/posterior boundary of the wing blade (Figure S1F). In contrast, cell death in *dlg-IR* wing discs was completely blocked in *egr*$^{-/-}$ animals (Figures 1B and S2C). Instead, the *dpp* domain was enlarged and 100% of *egr*$^{-/-}$; *dpp > dlg-IR*

animals died as pupae (n = 76) (Figure S1G). These results indicate that *egr*-dependent removal of *dlg*-deficient cells was beneficial for organism survival, consistent with the role of *egr* in *dlg* and *scrib* clone removal recently reported (Igaki et al., 2009). Surprisingly, we observed a similar requirement for *egr* in the phenotypes of whole animals who are deficient for *scrib* and *dlg* (Bilder and Perrimon, 2000). Patches of apoptosis in imaginal discs tumors and the characteristic larval arrest were suppressed in an $egr^{-/-}$ background (Figure S4). Most importantly, the epithelial delamination/migration phenotype of *dpp > dlg-IR* cells was also completely blocked in the absence of *egr*. The latter suggested that *egr* could promote tumor cell migration. We decided to further investigate such a potential role.

TNF Is Required for Extracellular Matrix, but Not Actin, Remodeling

Consistent with an involvement of JNK, reducing *dlg* function in the wing pouch (*sd > dlg-IR*) resulted in increased dMMP1 expression and MMP activity in situ (Figures 1D, 1G, and S3B). Importantly, the increased dMMP1 expression and MMP activity was fully dependent on *egr* (Figures 1E, 1H, and S3C). This indicates that the ability to disrupt tissue architecture by remodeling and crossing the basal membrane, a fundamental property of this neoplastic tumor suppressor, is not a necessary outcome of Dlg loss and instead requires *egr* activity. Another property associated with JNK activity and invasion is actin remodeling (Uhlirova and Bohmann, 2006) and indeed Dlg deficiency led to remodeling of actin fibers (Figures 1D–1H). Interestingly, eliminating *egr* had no drastic effect on *dlg*-dependent actin remodeling, suggesting that other pathways contribute to this process and this could be an intrinsic property of the loss of cell polarity.

Together, these results led us to speculate that *egr* could be involved in promoting tumor cell migration. Such a function of *egr* may be obscured by its own tumor suppressive role because *dlg*- and *scrib*-deficient cells die concomitantly on Egr signaling (Igaki et al., 2009). Furthermore, *dpp > dlg-IR* (Figure 1A) migrating cells were also eliminated by cell death. We then tested our hypothesis in conditions where cell migration/invasion are more favorable.

Ras Highjacks TNF Signaling

Overexpression of oncogenic Ras (Ras^{V12}) in discrete $scrib^{-/-}$ clones (Ras^{V12}; $scrib^{-/-}$) leads to invasive tumors (Pagliarini and Xu, 2003). We next explored the role of *egr* in this context using the MARCM system (Lee and Luo, 1999). Ras^{V12}; $scrib^{-/-}$ mutant eye-antennae patches were generated within genotypically $egr^{+/+}$ or $egr^{-/-}$ animals. $scrib^{-/-}$ patches were similarly generated as controls (Figure S5; data not shown). As anticipated, Ras^{V12}; $scrib^{-/-}$ eye-antennal clones developed into tumor-like growths with invasive migration into the ventral nerve cord (VNC) of the central nervous system (Figures 2C and 2E) (Igaki et al., 2006; Pagliarini and Xu, 2003; Uhlirova and Bohmann, 2006). We next examined the levels of dMMP1, as readout of JNK signaling (Bakal et al., 2008) required for invasive migration of Ras^{V12}; $scrib^{-/-}$ cells (Uhlirova and Bohmann, 2006). Early, small clones of Ras^{V12}; $scrib^{-/-}$ expressed high levels of dMMP1 throughout the clones (Figure S5G). However, such expression was observed primarily at the edges and invasive fronts of more mature tumors (Figures 2E, S5B, and S5E). This suggests that dMMP1 expression is not a necessary outcome in all Ras^{V12}; $scrib^{-/-}$ cells. Most animals (90.8%, n = 120) died as oversized larvae (Figures 2A and 2I).

Importantly, when generated in an $egr^{-/-}$ background, Ras^{V12}; $scrib^{-/-}$ clones displayed noninvasive overgrowth, failed to express dMMP1, and instead remained contained at their sites of origin within the eye-antennae discs (Figures 2D, 2F, S5C, and S5F). Furthermore, these Ras^{V12}; $scrib^{-/-}$; $egr^{-/-}$ animals progressed to the pupal stage (100%, n = 154) (Figures 2B and 2I).

As an additional readout of JNK activation we examined levels of dual phosphorylated JNK (p-JNK). As reported previously (Igaki et al., 2006), we observed ectopic p-JNK in Ras^{V12}; $scrib^{-/-}$ clones. However, similar to the expression of dMMP1, the high levels of p-JNK were regional (e.g., arrows in Figure 2G). Most importantly, we did not observe ectopic p-JNK in Ras^{V12}; $scrib^{-/-}$ clones in an $egr^{-/-}$ background (Figure 2H). This indicates that JNK activation, dMMP1 expression, and invasive migration in Ras^{V12}; $scrib^{-/-}$ cells required Egr signaling.

Therefore, *egr* plays a protumor role when oncogenic Ras is also provided to the cells. Moreover, *egr* provides a switch from noninvasive (in situ) to invasive *scrib* tumor growth in the presence of oncogenic Ras.

TNF Is Produced Non-Cell-Autonomously

In the search to understand the mechanisms mediating the role of *egr* we next examined the source of the endogenous Egr protein in Ras^{V12}; $scrib^{-/-}$ tumors.

Even though we were able to detect Egr in tumor cells, interestingly, Egr expression was highest in nontumoral cells that decorated the surface of the tumors (Figure 3A). We then went on to determine the identity of such Egr-expressing cells. Based on a proposed role of cell competition in the elimination of *scribble*-group cells (Uhlirova and Bohmann, 2006), and our previous speculations (Vidal and Cagan, 2006), the wild-type epithelial neighbors were primary candidates. However, although a role of such cells cannot be ruled out, the presence of *egr*-dependent apoptosis in tissues from animals fully deficient for Dlg or Scrib (Figure S4) indicated that the wild-type epithelial neighbors were not absolutely required for the initiation of Egr signaling.

TNF Is Produced by Tumor-Associated Hemocytes

In mammals, the association of immune cells to tumors is well-characterized (Siveen and Kuttan, 2009). Recent work in *Drosophila* demonstrated that hemocytes associate to Ras^{V12}; $scrib^{-/-}$ tumors (Pastor-Pareja et al., 2008). Additionally, crystal cells (a subtype of hemocytes) require *egr* for rupture (Bidla et al., 2007). We then considered that the Egr-expressing cells associated to Ras^{V12}; $scrib^{-/-}$ tumors could be hemocytes. We next stained the tissues for Nimrod C1, a marker for the plasmatocyte subtype of hemocytes (Kurucz et al., 2007) known to associate to Ras^{V12}; $scrib^{-/-}$ tumors (Pastor-Pareja et al., 2008). We observed numerous hemocytes associated to the tumors (Figure 3B). Interestingly, occasionally the tumor associated hemocytes (TAHs) displayed engulfed tumor cell fragments with apoptotic body-like morphology (arrow in Figure 3B′). TAHs were also observed in Ras^{V12}; $scrib^{-/-}$ clones in an $egr^{-/-}$ background (Figure 3C), suggesting that *egr* does not play an essential role in the association of hemocytes to tumors. Most importantly, by costaining with Nimrod C1 and Egr antisera, we observed that TAHs expressed high levels of Egr (Figure 3D). The expression of Egr was not observed in circulating hemocytes (Figure S7) or in hemocytes not associated to tumors (e.g., Figures 3E and 4B). Importantly, clones deficient for *lgl* also displayed associated hemocytes that expressed Eiger (Figure 4A). Furthermore, more hemocytes were found associated to Dlg-deficient wing pouches than to control discs (Figures 4C–4E).

Taken together, the data indicates that (1) hemocytes associate to cells deficient for scrib group genes; (2) Egr is expressed by TAHs; and (3) Egr expression in hemocytes and signaling activation are likely triggered on interaction of hemocytes with tumor cells.

Circulating Hemocytes Are Recruited to Tumors

Hemocytes have been found associated to imaginal discs from normal animals (Pastor-Pareja et al., 2008) (Figures 4B and 4C) Therefore, a key open question is whether TAHs originate from a population of residing hemocytes, or if they are instead recruited to the tumors from the population of circulating cells. To distinguish between these two possibilities we carried out hemolymph transfusion assays (see Experimental Procedures). We created animals with RFP-labeled hemocytes and transfused their hemolymph to animals bearing GFP-labeled, eye-antennae clones of Ras^{V12}; $scrib^{-/-}$ cells (Figure 5A). After a recovery period of 24 hr after the transfusion, we observed numerous RFP-labeled hemocytes recruited to Ras^{V12}; $scrib^{-/-}$ tumors (Figure 5F). Such ectopic hemocytes were mostly observed at the surface of the tumors (Figure 5F, inset), although we also observed RFP-labeled hemocytes completely embedded within the tumors (not depicted). Transfused hemocytes associated at a low frequency to clones of either wild-type, Ras^{V12}, $scrib^{-/-}$, or to $dlg-IR$ cells (Figures 5B–5E and data not depicted). Nevertheless, endogenous hemocytes associated to $lgl^{-/-}$, $scrib^{-/-}$, and $dlg-IR$ cells (Figures 4A, 4D, and 5G).

Together these results suggest that Ras^{V12}; $scrib^{-/-}$ tumors preferentially attracted and/or retained hemocytes from the circulation. On the other hand the low association of transfused circulating hemocytes to *scribble* group mutant patches suggests that: (1) hemocytes associated to such clones represent residing cells; or (2) there are technical limitations to our transfusion method (e.g., timing and sensitivity) that prevented us from assessing the contribution of circulating hemocytes in these contexts.

TNF Expression in Hemocytes Is Necessary

Because we found that Egr-expressing hemocytes associate to cells deficient for *scrib* group (Figures 3A, 3D, and 4A), we next examined the functional importance of Egr expression in these hemocytes. We created clonal patches of $lgl^{-/-}$ cells in developing wing discs in either a control background or a background in which the expression of Egr was specifically compromised in hemocytes ($he > egr-IR$) (see Figures S4I–S4L for validation of $egr-IR$). As expected, in the control background the $lgl^{-/-}$ cells were eliminated from the tissue by 72 hr after clonal induction (0 surviving clones/disc, n = 6 discs). Furthermore the discs displayed normal morphology and were composed exclusively of heterozygous cells and $lgl^{+/+}$ "twin spots" (Figure 6A, arrowheads). In contrast, in a $he > egr-IR$ background, numerous and large $lgl^{-/-}$ clones were observed (12.5 surviving clones/disc, n = 6 discs). Such clones displayed aberrant actin fibers (Figure 6C) and the wing discs showed abnormal morphology and ectopic folds (red arrow in Figure 6B). Adult eyes from clones created in the eye-antennae discs displayed characteristic patterning defects (Figure 6D) (Grzeschik et al., 2007). Importantly, in a $he > egr-IR$ background, this phenotype was enhanced markedly (Figure 6E).

These results indicate that the expression of Egr in hemocytes is necessary for the efficient removal of lgl cells.

TNF Expression in TAHs Is Sufficient for dMMP1 Expression in Tumors

Finally, we used the hemolymph transfusion technique to further test the functional importance of Egr expression in hemolymph cells. We observed that imaginal disc tumors from $scrib^{-/-}$ larvae ectopically expressed high levels of dMMP1 (Figure 7A), which was fully dependent on egr (Figure 7B). We then transfused hemolymph from either $egr^{+/+}$ or $egr^{-/-}$ animals into $scrib^{-/-}$ $egr^{-/-}$ animals. We observed a partial and regional rescue of dMMP1 expression by transfusing $egr^{+/+}$ hemolymph (Figure 7C), but not $egr^{-/-}$ hemolymph (Figure 7D). Similarly, we transfused hemolymph from $egr^{+/+}$ or $egr^{-/-}$ animals into animals with $egr^{-/-}$, Ras^{V12}; $scrib^{-/-}$ eye clones. The regional expression of

dMMP1 in $egr^{-/-}$, Ras^{V12}; $scrib^{-/-}$ clones was rescued in animals transfused with $egr^{+/+}$ hemolymph, but not in animals transfused with $egr^{-/-}$ hemolymph (Figures 7E and 7F).

Interestingly, when we used hemolymph from $egr^{+/+}$ animals with RFP-labeled hemocytes ($he > RFP$), we observed that the rescued expression of dMMP1 correlated with the association of $egr^{+/+}$ hemocytes. Clones of $egr^{-/-}$, Ras^{V12}; $scrib^{-/-}$ cells with TAHs expressed dMMP1 whereas nearby clones without TAHs did not (arrow and asterisk in Figure 7G, respectively). In large clones of $egr^{-/-}$, Ras^{V12}; $scrib^{-/-}$ cells, we observed that the expression of dMMP1 was highest in cells near the $egr^{+/+}$ TAHs and faded away on cells distant to the TAHs (Figure 7H).

Together, these results indicate that Egr expression in TAHs is sufficient to rescue the expression of dMMP1 in tumor cells.

DISCUSSION

TNF Can Act as a Tumor Promoter in Drosophila

The oncogenic cooperation of Ras^{V12} and tumor suppressors of the *scribble* group results in aggressive tumoral growth in *Drosophila* (Brumby and Richardson, 2003; Pagliarini and Xu, 2003). We believe this study shows that TNF/Egr is essential for the malignant progression of Ras^{V12}; $scrib^{-/-}$ tumors. In this context, the protumor role of TNF signaling has at least two components: (1) the host arrest in the larval stage, which allows an extended window of time for tumor progression; and (2) the activation of JNK in tumor cells, which in turns provides a switch from in situ to invasive growth.

A large body of research indicates that TNF can act as a tumor promoter in mammals (Balkwill, 2009). We show that such a tumor promoter role is conserved in flies. Importantly, although the contexts in which TNF acts as a tumor suppressor or tumor promoter in mammals are still poorly understood, we describe a genetically defined model in which the Ras oncogene mediates the switch from in situ to invasive growth by usurping TNF signaling in cells deficient for genes of the *scribble* group.

Hallmark Phenotypes of Scribble Group Genes Depend on TNF Signaling

The discovery of *lgl* mutants provided early evidence for the existence of tumor suppressor genes (Bridges and Brehme, 1944). However, the biological roles of the *scrib* group genes in cell polarity, proliferation, tissue architecture, and tumor suppression remain not fully understood. In this study, we provide evidence that TNF signaling is fundamentally involved in hallmark phenotypes of the *scrib* group genes. The characteristic larval arrest, disc overgrowth and ECM remodeling (partially responsible for disrupted tissue architecture) in *scrib* or *dlg* fully mutant animals were dependent on TNF. We speculate that the larval arrest may be caused by an attempt from the host to eliminate completely the presence of abnormal, potentially tumorigenic cells before progressing to the next developmental stage. In this view, TNF participates in a "developmental checkpoint" to secure the integrity of future adult tissues.

However, in the case *scrib* group-deficient cells became refractory to TNF-dependent death (e.g., by expressing the Ras oncoprotein), or in the case of fully mutant animals (i.e., composed exclusively of mutant cells), the targeted cells are never fully eliminated and instead usurp the larval arrest as an extended opportunity for tumoral growth.

Associated Hemocytes Trigger JNK Signaling

The JNK pathway plays an important role in *scrib* group mutant cells (Brumby and Richardson, 2005), but it is unclear how it is activated. It has been proposed previously that *scrib* group mutant cells are eliminated by JNK activation as a result of cell competition (Uhlirova and Bohmann, 2006). Also, JNK could mediate a stress response triggered by the loss of polarity (Bakal et al., 2008). We postulate an alternative, nonexclusive possibility: that JNK signaling in scrib group deficient cells is activated by a TNF-dependent cellular immune response from the host. Several lines of evidence support this possibility: (1) the ectopic JNK activation and expression of its target dMMP1 were regional; (2) TNF-dependence was maintained in fully deficient *scrib* group animals; (3) circulating hemocytes were recruited to *scrib*-deficient tumors and expressed Egr; (4) the survival of *lgl* clones improved when TNF expression was compromised specifically in hemocytes; and (5) the association of wild-type hemocytes was sufficient to rescue dMMP1 expression in TNF-deficient tumors.

The activation of JNK due to the loss of polarity has been observed in a highly sensitive cell culture-based assay (Bakal et al., 2008), and it is also likely that *scrib* group mutants do not have normal growth rates and thus engage in cell competition with neighbors. Therefore, we do not discard that these processes contribute to the phenotypes observed. Nevertheless, our data strongly indicate that TNF signaling triggered by interactions with TAHs is a major component of JNK activation and the phenotypes of *scrib* group cells.

Usurping the Host Immune Response

We propose a model (Figure 7I) in which TNF signaling is triggered in scrib group cells on interactions with TAHs. This mechanism perhaps evolved as a tumor suppressor function of the innate immune system and normally results in the apoptosis of the mutant—and potentially tumorigenic—cells and thus benefits host survival. However, in the case of oncogenic cooperation with Ras, the mutant cells highjack this immune response and redirect it to promote invasive growth and this acts in detriment of the host. In the absence of TNF, both $scrib^{-/-}$ and Ras^{V12}; $scrib^{-/-}$ cells developed as in situ outgrowths. This cooperation of Ras with TNF and related tumor associated inflammation suggests that the Ras oncoprotein provides an important selective advantage to tumors under attack from the host, and may account for the observation that Ras^{V12} is one of the most common activating mutations in human solid tumors. Furthermore, K-Ras strongly cooperates with forced inflammation in a murine model for pancreatic cancer (Guerra et al., 2007). Other oncogenic pathways capable of cooperating with *scrib* group genes, such as Notch (Brumby and Richardson, 2003), may result in a similar effect.

In mammalian tumors, TNF is produced by both the tumor cells and associated immune cells (Balkwill, 2009). The situation is similar in *Drosophila* because Igaki et al. (2009) reported that Egr acts in an intrinsic, cell autonomous fashion in *scrib* cells. In this study, we describe that TNF acted also in a non-cell-autonomous fashion. Indeed, TNF was expressed by TAHs and most importantly, TNF expressed in hemocytes was functionally relevant.

Implications for Human Cancer

Both protumor and antitumor activities of TNF and tumor-associated inflammation have been observed in murine models and the clinic (Balkwill, 2009). Although the importance of Ras in cancer is widely appreciated, the role of mammalian *scribble* group genes as tumor suppressors is just beginning to emerge (Humbert et al., 2008; Zhan et al., 2008). Given the striking conservation observed between the role of TNF in fly and vertebrate tumor models, we envision that our results could contribute to define key classifier genes and pathways that accurately predict the outcome of TNF signaling in the clinic.

EXPERIMENTAL PROCEDURES

Cultures

Cultures were carried out on semidefined medium (described by the Bloomington *Drosophila* stock center) at 25°C, except for the experiments shown in Figures 1A–1C and 5, which were carried out at 29°C. All initial *Drosophila* stocks used were described previously, except *UAS-dlg-IR^VDRC41136* and *UAS-egr-IR^VDRC42252*, stocks uncharacterized previously from the Vienna *Drosophila* RNAi collection (Dietzl et al., 2007).

Immunofluorescence

Immunofluorescence was carried out as described (Brachmann et al., 2000). Antibodies were anticleaved caspase 3 (1:100, Cell Signaling), anti-Dlg (1:500, DSHB), anti-dMMP1 (1:10, DSHB), anti-Laminin B1 (1:40, Abcam), anti-NimC1 P1 (Kurucz et al., 2007), anti-pJNK G9 (1:100, Cell Signaling), and anti-Egr (Igaki et al., 2009). Actin fibers were visualized with rhodamine/phalloidin (1:50, Molecular Probes). Secondary antibodies were Alexa-conjugated 488, 568, or 633 (Molecular Probes).

Collagenase/Gelatinase Activity In Situ and Imaging

Dissected wing imaginal discs were incubated immediately in 100 μg/mL DQ gelatin (FITC-conjugated, Molecular Probes) in PBS for 40 min at room temperature. Tissues were transferred to fixative solution (4% formaldehyde in PBS) for 30 min at 0°C. No background signal was observed in tissues that were fixed before incubation with DQ gelatin (data not shown). Whole animal micrographs were taken with a Leica Z16 stereomicroscope with Montage software. Confocal images were obtained with a Leica DM500 or Nikon A1R confocal microscopes. Experimental and controls were imaged using identical microscope settings, n ≥ 8 for all experiments. Phenotype frequencies were scored at ≥12 days AED. Note that larval life normally ends at Day 4–5 AED; larvae that were ≥12 days old displayed a drastic larval arrest phenotype.

Wing Disc Size

The sizes in two dimensions were measured by transferring four wing discs per slide, and covering with 20 × 60 mm coverslides. Confocal projections were obtained and analyzed with Image J software.

Statistical Analysis

We used Student's t test for disc size measurements and nonparametric Mann-Whitney test for hemocyte association, as the data distribution were not normal.

Live Visualization

Discs were cultured apical-side-down in Schneider's Insect culture media (S2 media) on a glass bottom dish and visualized on a inverted confocal microscope.

Hemolymph Transfusion

All solutions and tools were sterile. Glass capillaries (1.0 mm outer diameter, 0.78 mm inner diameter) were pulled with a P-30 Needle puller (Sutter Instruments) and broken at ~0.5 mm from the tip. Larvae were rinsed in S2 media and anesthetized with CO_2. "Donor" larvae were dried and opened with micro-forceps with care not to damage internal tissues. Four to eight larvae were grouped together. Their hemolymph was loaded immediately into the micro needle by using a Narishige 1M-5A manual microinjector and transfused within 5 min to avoid melanization and hemocyte adhesion to available surfaces. "Acceptor" larvae were

injected ~0.75 µl at the posterior one-third on the ventral side and transferred into a culture vial with excess humidity to recover for 24 hr. Larvae that died or that displayed excessive melanization after the transfusion were discarded.

Supplementary Material

Refer to Web version on PubMed Central for supplementary material.

Acknowledgments

References

Bakal C, Linding R, Llense F, Heffern E, Martin-Blanco E, Pawson T, Perrimon N. Phosphorylation networks regulating JNK activity in diverse genetic backgrounds. Science. 2008; 322:453–456. [PubMed: 18927396]

Balkwill F. Tumour necrosis factor and cancer. Nat Rev Cancer. 2009; 9:361–371. [PubMed: 19343034]

Balkwill FR, Lee A, Aldam G, Moodie E, Thomas JA, Tavernier J, Fiers W. Human tumor xenografts treated with recombinant human tumor necrosis factor alone or in combination with interferons. Cancer Res. 1986; 46:3990–3993. [PubMed: 2425938]

Bidla G, Dushay MS, Theopold U. Crystal cell rupture after injury in *Drosophila* requires the JNK pathway, small GTPases and the TNF homolog Eiger. J Cell Sci. 2007; 120:1209–1215. [PubMed: 17356067]

Bilder D, Perrimon N. Localization of apical epithelial determinants by the basolateral PDZ protein Scribble. Nature. 2000; 403:676–680. [PubMed: 10688207]

Brachmann CB, Jassim OW, Wachsmuth BD, Cagan RL. The *Drosophila* Bcl-2 family member dBorg-1 functions in the apoptotic response to UV-irradiation. Curr Biol. 2000; 10:547–550. [PubMed: 10801447]

Brand AH, Perrimon N. Targeted gene expression as a means of altering cell fates and generating dominant phenotypes. Development. 1993; 118:401–415. [PubMed: 8223268]

Bridges, CB.; Brehme, KS. The Mutants of *Drosophila melanogaster*. Washington, DC: Carnegie Institute; 1944.

Brumby AM, Richardson HE. scribble mutants cooperate with oncogenic Ras or Notch to cause neoplastic overgrowth in *Drosophila*. EMBO J. 2003; 22:5769–5779. [PubMed: 14592975]

Brumby AM, Richardson HE. Using *Drosophila melanogaster* to map human cancer pathways. Nat Rev Cancer. 2005; 5:626–639. [PubMed: 16034367]

Dietzl G, Chen D, Schnorrer F, Su KC, Barinova Y, Fellner M, Gasser B, Kinsey K, Oppel S, Scheiblauer S, et al. A genome-wide transgenic RNAi library for conditional gene inactivation in *Drosophila*. Nature. 2007; 448:151–156. [PubMed: 17625558]

Grzeschik NA, Amin N, Secombe J, Brumby AM, Richardson HE. Abnormalities in cell proliferation and apico-basal cell polarity are separable in *Drosophila* lgl mutant clones in the developing eye. Dev Biol. 2007; 311:106–123. [PubMed: 17870065]

Guerra C, Schuhmacher AJ, Canamero M, Grippo PJ, Verdaguer L, Perez-Gallego L, Dubus P, Sandgren EP, Barbacid M. Chronic pancreatitis is essential for induction of pancreatic ductal adenocarcinoma by K-Ras oncogenes in adult mice. Cancer Cell. 2007; 11:291–302. [PubMed: 17349585]

Humbert PO, Grzeschik NA, Brumby AM, Galea R, Elsum I, Richardson HE. Control of tumorigenesis by the Scribble/Dlg/Lgl polarity module. Oncogene. 2008; 27:6888–6907. [PubMed: 19029932]

Igaki T, Kanda H, Yamamoto-Goto Y, Kanuka H, Kuranaga E, Aigaki T, Miura M. Eiger, a TNF superfamily ligand that triggers the *Drosophila* JNK pathway. EMBO J. 2002; 21:3009–3018. [PubMed: 12065414]

Igaki T, Pagliarini RA, Xu T. Loss of cell polarity drives tumor growth and invasion through JNK activation in *Drosophila*. Curr Biol. 2006; 16:1139–1146. [PubMed: 16753569]

Igaki T, Pastor-Pareja JC, Aonuma H, Miura M, Xu T. Intrinsic tumor suppression and epithelial maintenance by endocytic activation of Eiger/TNF signaling in *Drosophila*. Dev Cell. 2009; 16:458–465. [PubMed: 19289090]

Kurucz E, Markus R, Zsamboki J, Folkl-Medzihradszky K, Darula Z, Vilmos P, Udvardy A, Krausz I, Lukacsovich T, Gateff E, et al. Nimrod, a putative phagocytosis receptor with EGF repeats in *Drosophila* plasmatocytes. Curr Biol. 2007; 17:649–654. [PubMed: 17363253]

Lee T, Luo L. Mosaic analysis with a repressible cell marker for studies of gene function in neuronal morphogenesis. Neuron. 1999; 22:451–461. [PubMed: 10197526]

Moore RJ, Owens DM, Stamp G, Arnott C, Burke F, East N, Holdsworth H, Turner L, Rollins B, Pasparakis M, et al. Mice deficient in tumor necrosis factor-alpha are resistant to skin carcinogenesis. Nat Med. 1999; 5:828–831. [PubMed: 10395330]

Moreno E, Yan M, Basler K. Evolution of TNF signaling mechanisms: JNK-dependent apoptosis triggered by Eiger, the *Drosophila* homolog of the TNF superfamily. Curr Biol. 2002; 12:1263–1268. [PubMed: 12176339]

Page-McCaw A, Serano J, Sante JM, Rubin GM. *Drosophila* matrix metalloproteinases are required for tissue remodeling, but not embryonic development. Dev Cell. 2003; 4:95–106. [PubMed: 12530966]

Pagliarini RA, Xu T. A genetic screen in *Drosophila* for metastatic behavior. Science. 2003; 302:1227–1231. [PubMed: 14551319]

Pastor-Pareja JC, Wu M, Xu T. An innate immune response of blood cells to tumors and tissue damage in *Drosophila*. Dis Model Mech. 2008; 1:144–154. discussion 153. [PubMed: 19048077]

Perrimon N. The maternal effect of lethal(1)discs-large-1: a recessive oncogene of *Drosophila melanogaster*. Dev Biol. 1988; 127:392–407. [PubMed: 3132409]

Siveen KS, Kuttan G. Role of macrophages in tumour progression. Immunol Lett. 2009; 123:97–102. [PubMed: 19428556]

Uhlirova M, Bohmann D. JNK- and Fos-regulated Mmp1 expression cooperates with Ras to induce invasive tumors in *Drosophila*. EMBO J. 2006; 25:5294–5304. [PubMed: 17082773]

Vidal M, Cagan RL. *Drosophila* models for cancer research. Curr Opin Genet Dev. 2006; 16:10–16. [PubMed: 16359857]

Zhan L, Rosenberg A, Bergami KC, Yu M, Xuan Z, Jaffe AB, Allred C, Muthuswamy SK. Deregulation of scribble promotes mammary tumorigenesis and reveals a role for cell polarity in carcinoma. Cell. 2008; 135:865–878. [PubMed: 19041750]
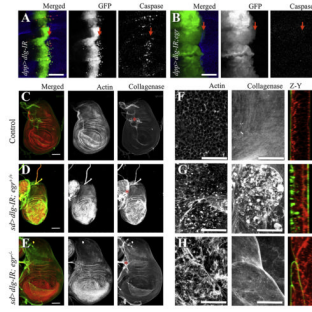
Figure 1. Dlg-Deficient Cell Delamination and ECM Remodeling Are *egr*-Dependent
Confocal images from larval wing discs. Full genotypes for all figures are described in Supplemental Experimental Procedures; relevant genotypes are indicated. In (A) and (B), arrows indicate anterior/posterior (A/P) boundary; the *dpp* expression domain is an anterior stripe at the boundary. Left panels are color overlays from GFP (green), cleaved caspase-3 (red) fluorescent signals; the remaining columns show individual stains in gray as labeled. (C–H) *sd-gal4* was used to drive expression of *dlg-IR* in the wing pouch region from the discs with the indicated *egr* background for each row of panels. Discs were stained for actin filaments (red and center column in C–E, left column in F–H) and collagenase/gelatinase activity in situ to visualize MMP activity (green and right column in C–E, center column in F–H). The right column in (F–H) displays optical cross sections along the Z and Y planes. Asterisks label overlaying trachea branches. Scale bars = (A) and (B), 150 μm, (C)–(E), 100 μm, and (F)–(H), 25 μm. See also Figures S1, S2, and S3.
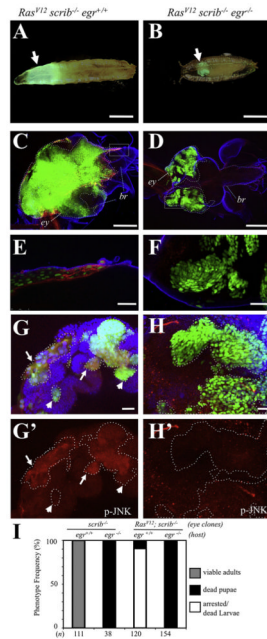
Figure 2. *egr* Is a Tumor Promoter in *Ras-scrib* Oncogenic Cooperation
GFP-labeled clones of cells with the following relevant genotypes were created in developing eye-antennae discs: (A, C, E, and G) Ras^{V12}; $scrib^{-/-}$ clones in $egr^{+/+}$ host; (B, D, F, and H) Ras^{V12}; $scrib^{-/-}$ clones in $egr^{-/-}$ host. (A) and (B) display the most frequent whole-animal phenotypes for the indicated genotypes. (C) and (D) display larval cephalic complexes labeled for GFP (green), dMMP1 (red), and Laminin B1 (blue); eye-antennae discs (*ey*) and brains (*br*) were outlined with white and blue dotted lines, respectively. (E) and (F) are high magnification views from the boxed area in (C) and (D), respectively. (G) and (H) display overlays for GFP (green), p-JNK (red), and DAPI (blue). Clones were outlined with dotted lines, and p-JNK stains are shown individually in (G′) and (H′). Arrows point to regions of Ras^{V12}; $scrib^{-/-}$ clones with high levels of p-JNK, whereas arrowheads point to regions with relative low levels of p-JNK. Scale bars = (A) and (B), 1 mm, (C) and (D), 200 μm, (E) and (F), 25 μm, and (G) and (H), 20 μm. (I) Phenotype frequencies for the relevant genotypes indicated on top of each column. The number of animals counted is displayed at the bottom. Note that animals with $scrib^{-/-}$ eye-antennae clones reached adulthood (100%, n = 111) in an $egr^{+/+}$ background but died during the pupa stage in an $egr^{-/-}$ background (100%, n = 38). In contrast, most animals (90.8%, n = 120) with Ras^{V12}; $scrib^{-/-}$ eye-antennae clones died at the (arrested) larva stage and displayed extensive tumors that invaded the brain in an $egr^{+/+}$ background (A, C, and E) but progressed toward the pupa stage and displayed in situ outgrowths in an $egr^{-/-}$ background (100%, n = 154, B, D, and F). See also Figures S4–S6.
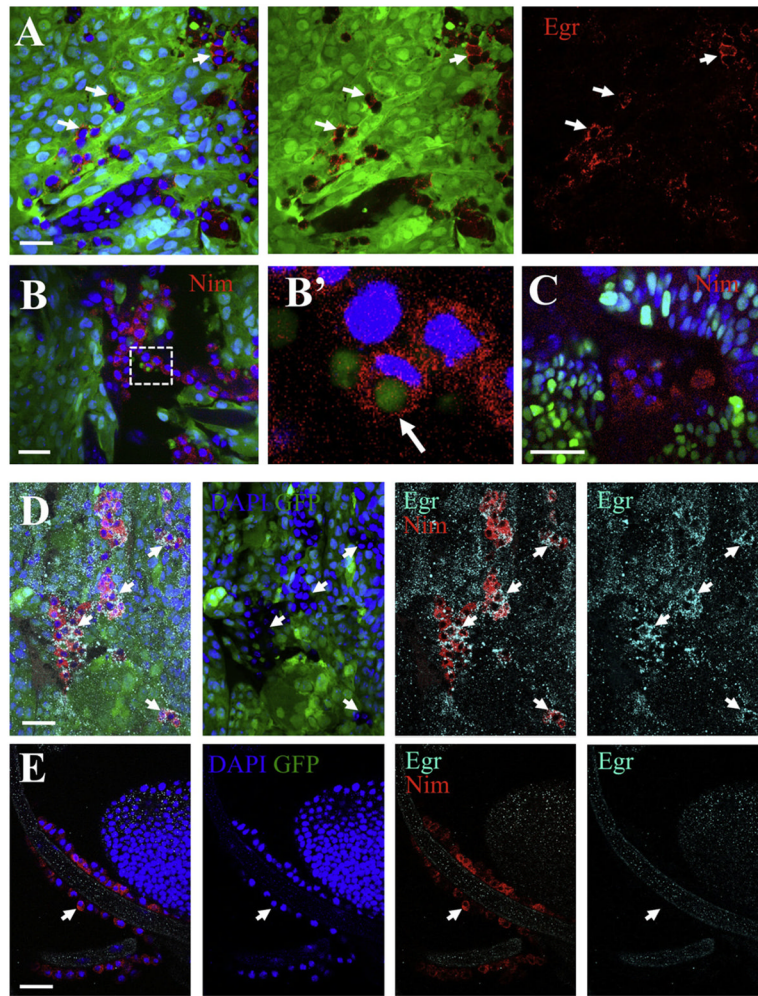
Figure 3. Associated Hemocytes Express Eiger
In all panels, GFP-labeled clones (green) of Ras^{V12}; $scrib^{-/-}$ cells were created in developing eye-antennae discs in $egr^{+/+}$ hosts, except in (C) where the host was $egr^{-/-}$. DAPI labeled nuclei are shown in blue. (A) Anti-Eiger (red) in Ras^{V12}; $scrib^{-/-}$ clones indicated that some tumor-associated cells express Eiger (arrows). (B and C) Anti-Nimrod C1 staining (Nim, red) labeled tumor-associated hemocytes. (B′) shows a high magnification view from the boxed area in (B). The arrow points to a phagocytosed tumor cell fragment. (D and E) Anti-Nimrod C1 (red) and Anti-Eiger (cyan) staining from a tumor (D) and a trachea branch (E) from the same animal. Left panels are merged images; the other panels show stains as labeled. Arrows point to hemocytes. Scale bars = (A), (B), (D), and (E), 20 μm, and (C), 25 μm. See also Figure S7.
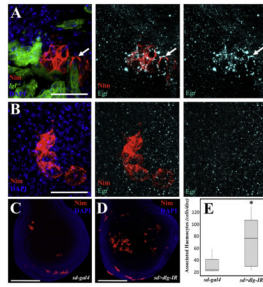
Figure 4. Hemocytes Associate to Lgl- and Dlg-Deficient Cells

(A) GFP-labeled Clonal patches of $lgl^{-/-}$ cells were created in developing wings. The tissues were stained for DAPI (blue), Nimrod C1 (red) and Eiger (cyan). The three panels show stains as labeled. The arrow points to an example of an Eiger-expressing hemocyte. Scale bar = 20 μm.

(B) Hemocytes were found associated to wild-type discs but did not express Eiger. Scale bar = 20 μm.

(C and D) Nimrod staining in *sd-gal* (C) and *sd > dlg-IR* (D) discs. Scale bars = 150 μm.

(E) Box plot quantification for the number of associated hemocytes in (C) and (D). The asterisk means statistical significance (p = 0.0385) in a nonparametric Mann-Whitney test (n = 6 and 9 for *sd-gal4* and *sd > dlg-IR*, respectively).
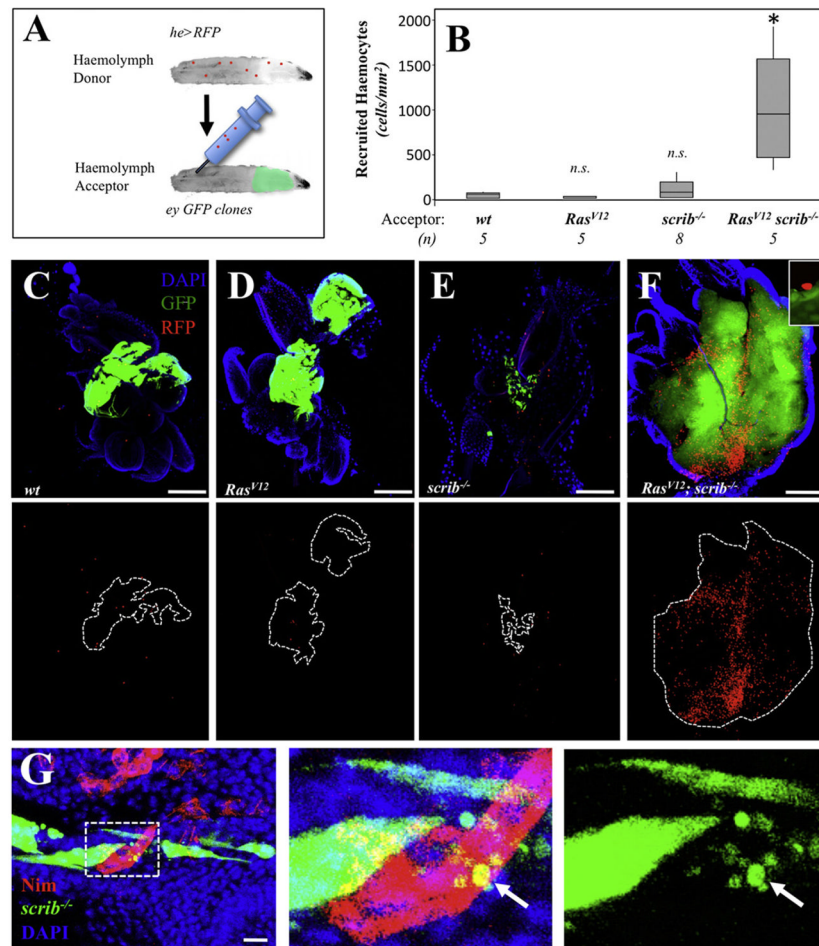
Figure 5. Ras^{V12}; $scrib^{-/-}$ Clones Recruit Hemocytes from the Circulating Population
(A) Schematic representation for the hemolymph transfusion assay. See Experimental Procedures for details.
(B) Box plot quantification for the number of transfused hemocytes associated to the clones with the indicated genotypes. The number of animals analyzed is indicated (n). The asterisk means statistical significance (p = 0.0122) in a nonparametric Mann-Whitney test (n.s. = nonstatistically significant).
(C–F) Representative Images from the transfusion experiments. The bottom panels display the transfused hemocytes in red and dotted lines outline of the clones. Scale bars = 100 μm.
(G) Anti-Nimrod C1 staining (red) from discs with GFP labeled $scrib^{-/-}$ clones. The center and right panels show high magnification views from the boxed area in (G). The arrow points to a phagocytosed tumor cell fragment. Scale bar = 10 μm.
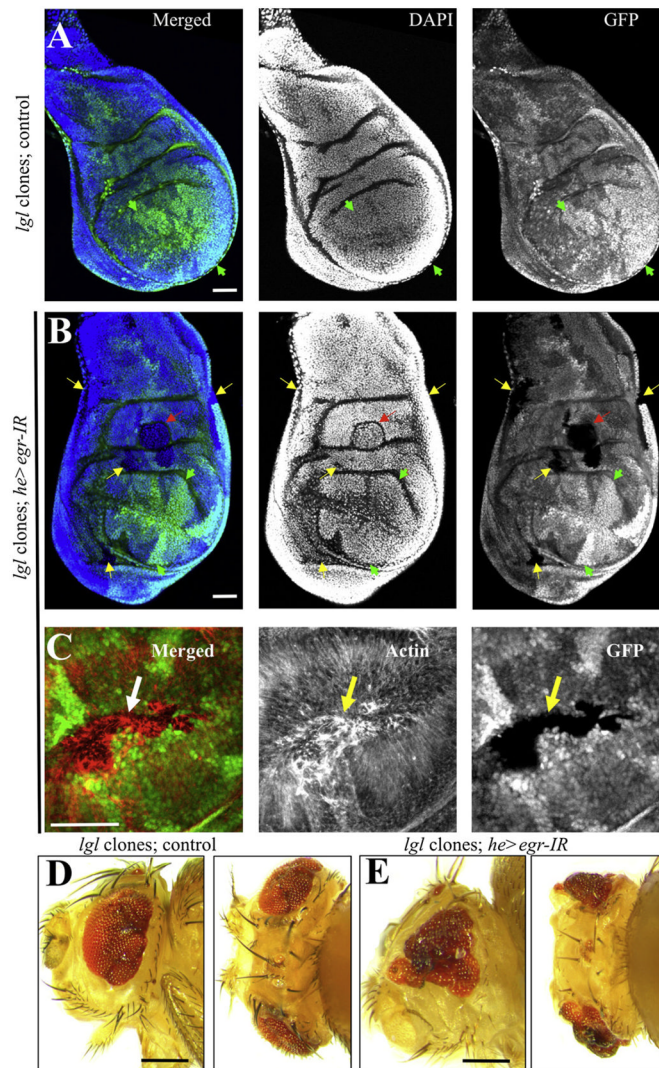
Figure 6. Eiger Expression in Hemocytes Is Required to Eliminate *lgl* Clones
Clonal patches of *lgl*$^{-/-}$ cells were created in developing (A–C) wing or (D and E) eye-antenna discs either in a (A, D) control genetic background, or (B, C, and E) in a background in which Eiger was specifically knocked-down in hemocytes (*he > egr-IR*). In (A) and (B), the left panels are overlays of DAPI staining for nuclei (blue) and GFP (green) to visualize clones. In (C), the left panel shows an overlay of actin fiber staining (red) and GFP (green). Each stain is also shown individually in gray. Wild-type (*lgl*$^{+/+}$) "twin spots" have high levels of GFP expression (e.g., green arrowheads). Yellow arrows in (B) and (C) point to some of the *lgl*$^{-/-}$ patches of cells that had no GFP expression. The red arrow in (B) points to a clone that created an ectopic fold in the tissue. (D) and (E) show adult heads from lateral (left) and top (right) views from animals with the indicated relevant genotypes. Scale bars = (A–C), 50 μm, (D and E); 250 μm.
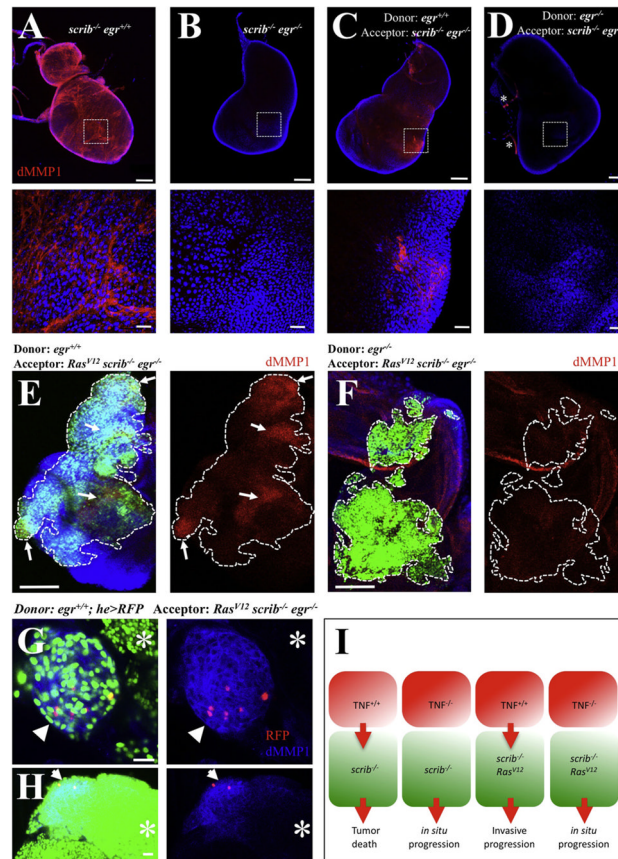
Figure 7. Eiger Expression in Hemocytes Is Sufficient for dMMP1 Expression in Tumor Cells
(A–D) dMMP1 (red) and DAPI (blue) stainings from imaginal disc tumors from $scrib^{-/-}$ larvae. The bottom panels show high magnification views from the boxed areas in the top panels. (A) Scrib-deficient discs displayed high levels of dMMP1. (B) dMMP1 expression was absent in $scrib^{-/-}$; $egr^{-/-}$ double mutant discs. (C) dMMP1 expression was partly and regionally rescued by transfusing wild-type hemolymph, but not $egr^{-/-}$hemolymph. (D) Asterisks label overlaying trachea branches, known to express endogenous dMMP1.
(E–H) GFP-labeled clones of Ras^{V12}; $scrib^{-/-}$ cells were created in developing eye-antennae discs in $egr^{-/-}$ hosts. The animals were transfused with the hemolymph from (E) $egr^{+/+}$, (F) $egr^{-/-}$, and (G and H) $egr^{+/+}$; $he > RFP$ animals. In (E) and (F), the left panels show an overlay from GFP (green), DAPI (blue), and dMMP1 (red). The dMMP1 stains are also shown individually. Dotted lines outline GFP-labeled clones and the arrows point to regions of rescued dMMP1 expression within the clones. In (G) and (H), left panels display overlays from GFP (green), dMMP1 (blue), and RFP (red). The right panels show overlays of the dMMP1 and RFP signals. The arrows point to clone or clone regions with high levels of dMMP1 expression, whereas the asterisks mark clone or clone regions with relative low levels of dMMP1. Scale bars = (A–D) top, (E), and (F), 100 μm, and (A–D) bottom, (G), and (H), 20 μm.
(I) Model for the switch of TNF signaling from anti- into protumor. Red cells represent tumor-associated hemocytes and the green ones cells deficient for genes of the *scribble* group. See the text for details.